Chinese Journal of Oceanology and Limnology
Vol. 35 No. 5, P. 1018-1031, 2017
http://dx.doi.org/10.1007/s00343-017-6082-9

Correspondence between the ENSO-like state and glacial-interglacial condition during the past 360 kyr*

ZHANG Shuai (张帅)[1, 3], LI Tiegang (李铁刚)[2, 4, **], CHANG Fengming (常凤鸣)[1, 4], YU Zhoufei (俞宙菲)[1, 2], XIONG Zhifang (熊志方)[1, 4], WANG Haixia (王海霞)[5]

[1] *Key Laboratory of Marine Geology and Environment, Institute of Oceanology, Chinese Academy of Sciences, Qingdao 266071, China*

[2] *Key Laboratory of Marine Sedimentology and Environmental Geology, First Institute of Oceanography, State Oceanic Administration (SOA), Qingdao 266061, China*

[3] *University of Chinese Academy of Sciences, Beijing 100049, China*

[4] *Laboratory for Marine Geology, Qingdao National Laboratory for Marine Science and Technology, Qingdao 266061, China*

[5] *Ningbo City Land Resources Bureau Yinzhou Branch, Ningbo 315100, China*

Received Mar. 16, 2016; accepted in principle May 18, 2016; accepted for publication Jul. 11, 2016

Abstract In the warming world, tropical Pacific sea surface temperature (SST) variation has received considerable attention because of its enormous influence on global climate change, particularly the El Niño-Southern Oscillation process. Here, we provide new high-resolution proxy records of the magnesium/calcium ratio and the oxygen isotope in foraminifera from a core on the Ontong-Java Plateau to reconstruct the SST and hydrological variation in the center of the Western Pacific Warm Pool (WPWP) over the last 360 000 years. In comparison with other Mg/Ca-derived SST and $\delta^{18}O$ records, the results suggested that in a relatively stable condition, e.g., the last glacial maximum (LGM) and other glacial periods, the tropical Pacific would adopt a La Niña-like state, and the Walker and Hadley cycles would be synchronously enhanced. Conversely, El Niño-like conditions could have occurred in the tropical Pacific during fast-changing periods, e.g., the termination and rapidly cooling stages of interglacial periods. In the light of the sensitivity of the Eastern Pacific Cold Tongue (EPCT) and the inertia of the WPWP, we hypothesize an inter-restricted relationship between the WPWP and EPCT, which could control the zonal gradient variation of SST and affect climate change.

Keyword: Western Pacific Warm Pool (WPWP); sea surface temperature (SST); El Niño-Southern Oscillation (ENSO)

1 INTRODUCTION

The Western Pacific Warm Pool (WPWP) constitutes the largest source of water vapor and heat for driving global atmospheric circulation (Cane, 1998) (Fig.1), and its air-sea interaction is significant in triggering El Niño-Southern Oscillation (ENSO) events (Sun, 2003). Spatial variation and hydrological status of the WPWP also affect Intertropical Convergence Zone (ITCZ) alteration and East Asian Monsoon intensity (Li et al., 1999; Leduc et al., 2009; Schmidt and Spero, 2011; Zhang et al., 2015). Interannual-scale precipitation in the WPWP is tightly coupled with the seasonal swing of the ITCZ and boreal winter monsoon cold wave variation (An, 2000). Some global ocean-atmosphere coupled models have shown that the evolution of the mode of atmospheric circulation is very sensitive to subtle variations of sea surface temperature (SST) in the WPWP, especially at high SSTs (Palmer and Mansfield, 1984; Ravelo et al., 1990). Modern satellite observations show that the SST and scale change of the WPWP is related to solar irradiance

* Supported by the Knowledge Innovation Engineering Project of Chinese Academy of Sciences (No. XDA10010305), the National Special Project for 'Global Change and Air-Sea Interaction' (No. GASI-04-01-02), and the National Natural Science Foundation of China (Nos. 41230959, 41076030, 41576051)
** Corresponding author: tgli@fio.org.cn

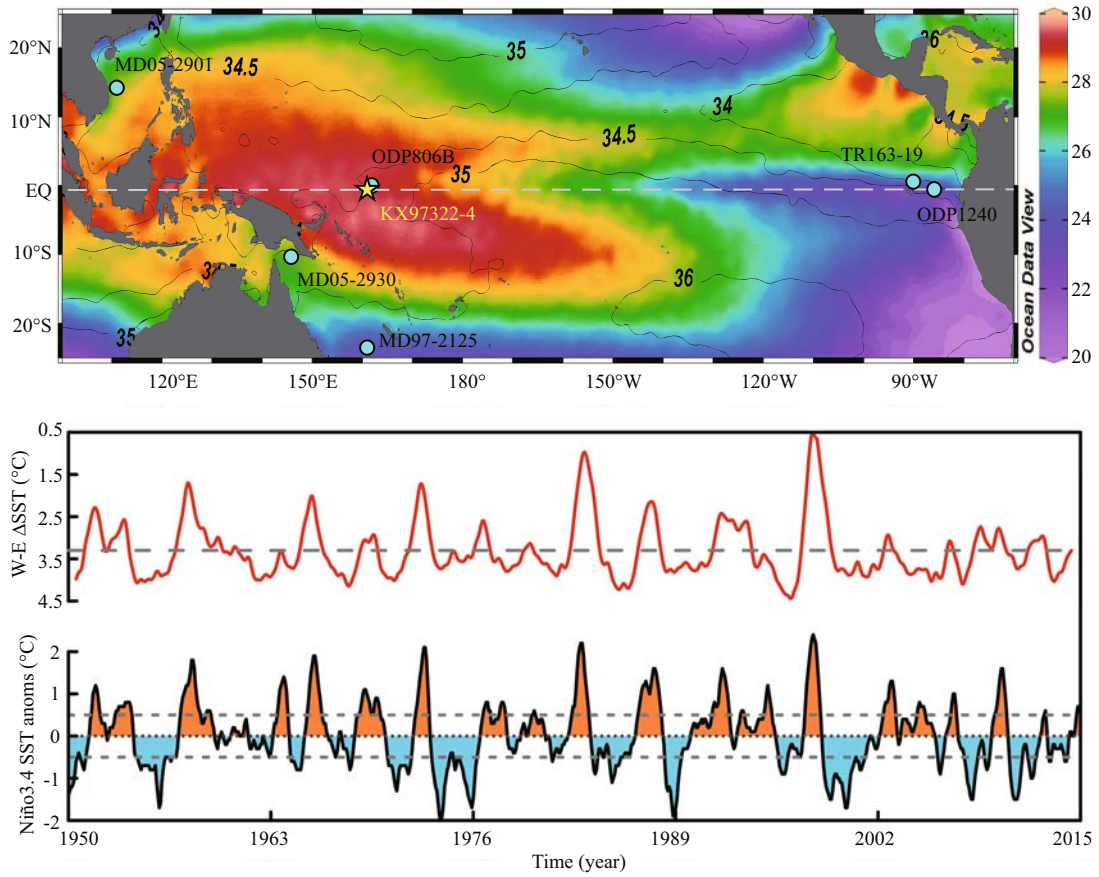

Fig.1 (Upper) map of average annual SST (°C) (color) and SSS (contour) of tropical Pacific, and the locations of core KX97322-4 (yellow star) and the other main cores mentioned (blue cycles) in this paper (top). SST and SSS data were taken from WOA13 (Schlitzer, 2015); (lower) comparison between west-east tropical Pacific SST difference and Niño 3.4 SST anomalies from 1950

The Niño 3.4 index data comprise 3-month running means of ERSST.v4 SST anomalies in the Niño 3.4 region, obtained from http://www.cpc.ncep.noaa.gov. SST data of WPWP (0°N, 160°E) and EPCT (2°N, 270°E), obtained from http://www.esrl.noaa.gov, were also calculated as 3-month running means.

variabilities, ENSO events, volcanic activities, and global warming (Yan et al., 1992).

Modern ENSO events in the tropical Pacific are important for global climate variation (Jin, 1996; Cane, 1998; Thunell et al., 1999; Fedorov and Philander, 2000; Cai et al., 2014). Furthermore, ENSO-like states or super-ENSO events have also appeared in past long-term variations (Lea et al., 2000; Stott et al., 2002; Cobb et al., 2013; Carré et al., 2014; Ford et al., 2015). The zonal SST gradient is an essential indicator for evaluating an ENSO event (Jin, 1996; Lea et al., 2000). Therefore, determining SST variation in the WPWP is crucial to the understanding of global climate change (Cronin and McPhaden, 1997). On long time scales, SST change in the WPWP is driven by orbital parameters, such as eccentricity, obliquity, and precession (Clement et al., 1999). To understand the tendency of ENSO variation, it is necessary to accumulate long-term continuous multiproxy records of SST to reconstruct the evolution of past ENSO-like or super-ENSO (Rosenthal and Broccoli, 2004).

Controversies remain to be resolved regarding the complex hydrological variation in the WPWP during past glacial-interglacial cycles because of the influences of ENSO-like processes, low-latitude monsoonal variation, ITCZ swing, and their interactions (Leduc et al., 2009; Cobb et al., 2013; Qiu et al., 2014a). For instance, different results obtained from various transfer function techniques and proxies, e.g., the Mg/Ca paleothermometer of planktic foraminiferal calcite (Crowley, 2000; de Garidel-Thoron et al., 2007; MARGO Project Members, 2009; Mathien-Blard and Bassinot, 2009) and clumped isotopes (Tripati et al., 2014), mean that the estimated amplitude of cooling in the WPWP during the Last Glacial Maximum (LGM) is inconsistent. Reconstruction of SST in the WPWP by Mg/Ca has

indicated an El Niño-like state in the tropical Pacific during the LGM (Koutavas et al., 2002). However, LGM SSTs, obtained from alkenone unsaturation in the East Pacific Cold Tongue (EPCT), appear to indicate local cooling, and upwelling intensified by enhanced trade winds over the eastern equatorial Pacific (EEP), which are suggestive of a La Niña-like state (Dubois et al., 2009). Multicore analyses of planktic foraminifera from the EEP indicate that the zonal gradient of SST was enhanced during the LGM (Andreasen and Ravelo, 1997; Martínez et al., 2003), while other results from the WPWP indicate the opposite (Sagawa et al., 2012; Ford et al., 2015). Based on a multiproxy record in the heart of the WPWP, de Garidel-Thoron et al. (2007) found no evidence of ENSO-like events during the last deglaciation. In addition, the migration of the ITCZ, which is controlled by the meridional SST gradient, also affects the hydrological variation in the WPWP and East Asian Monsoon activities. However, the relationship between the ITCZ and ENSO remains ambiguous (Schmidt and Spero, 2011; Zhang et al., 2015).

Given all the contradictions above, further research is needed to ascertain the role of the tropical Pacific in past climate change. This paper presents a series of geochemical proxy records of foraminifera from the center of the WPWP to reconstruct the hydrological variation of the WPWP during the past 360 000 years. We also discuss past ENSO-like processes and analyze the mechanism of paleoclimate change by comparison with other results.

2 MATERIAL AND METHOD

2.1 Sediment samples

Core KX97322-4 was obtained from the Ontong-Java Plateau (00°01.73′S, 159°14.66′E, water depth: 2 362 m, core length: 6.3 m; Fig.1) using a giant piston corer on board R/V *Science-1* during the Warm Pool Subject Cruise in 2008. The sediments of this core are composed mainly of calcium carbonate with little dissolution (the lysocline depth is 3 500 m in this area) (Wu and Berger, 1991; Sadekov et al., 2010).

The Ontong-Java Plateau area is located to the northeast of Papua New Guinea, in the center of the WPWP, within the sea surface isothermal line of 29°C (Fig.1). This region is perennially warm without obvious seasonal temperature or salinity variations (less than 1.3°C and 0.2, respectively). Seasonal fluctuation of precipitation in the WPWP is controlled by the coupled system of the Asian-Australian monsoon and the ITCZ, while its interannual variation is controlled by ENSO and the Indian Ocean Dipole system. Changes in the ITCZ and ENSO are induced primarily by solar forcing (Oppo et al., 2007; Schmidt and Spero, 2011), which is also the dominant factor controlling the intensity of the low-latitude summer monsoon. The interannual SST difference between the center of the WPWP and the EEP from 1950 to present (Version 4, in situ only) is in line with the Niño 3.4 SST anomalies (Fig.1); thus, it is a good indicator of past ENSO events.

2.2 Oxygen isotope and Mg/Ca analyses

The entire sediment core was sampled at 1-cm intervals. These samples were washed through a 63-μm sieve and dried at 60°C. Then, approximately 4–7 specimens of benthic foraminifera *Cibicidoides wuellerstorfi* were selected from the 355–500-μm size fraction for oxygen isotope analysis, and approximately 40 specimens of planktic foraminifera *Globigerinoides ruber* (white) were selected from the 250–300-μm size fraction for both oxygen isotope and Mg/Ca analyses. All the geochemical analyses were performed at the Institute of Oceanology of the Chinese Academy of Sciences. Foraminiferal shells were crushed under a microscope before cleaning.

The crushed foraminiferal shells used for the stable isotope analysis were sonicated in both 3% peroxide and acetone before being washed with distilled water and dried at 60°C. The oxygen isotope ratio was measured using a GV IsoPrime mass spectrometer. The analytical precision was not less than 0.06‰ (1σ). Calibration to VPDB was performed using standard NBS18.

The Mg/Ca cleaning procedure was based on the treating processes without a reductive step (Barker et al., 2003), because the planktic foraminifera *G. ruber* shells in this core are pristine. As the sample site is located far from the continent, there is no visible contamination by Iron-Manganese clastics, as observed during visual examination under a microscope. The Mg/Ca ratio was measured using Inductively Coupled Plasma-Optical Emission Spectrometry (ICP-OES, iCAP6300 radial; Thermo-Fisher). The analytical precision of the Mg/Ca ratio was 0.44% (1σ, RSD).

2.3 SST and SSS calculations

Previous studies have clarified a stable relationship between the Mg/Ca ratio of shells and ambient water temperature:

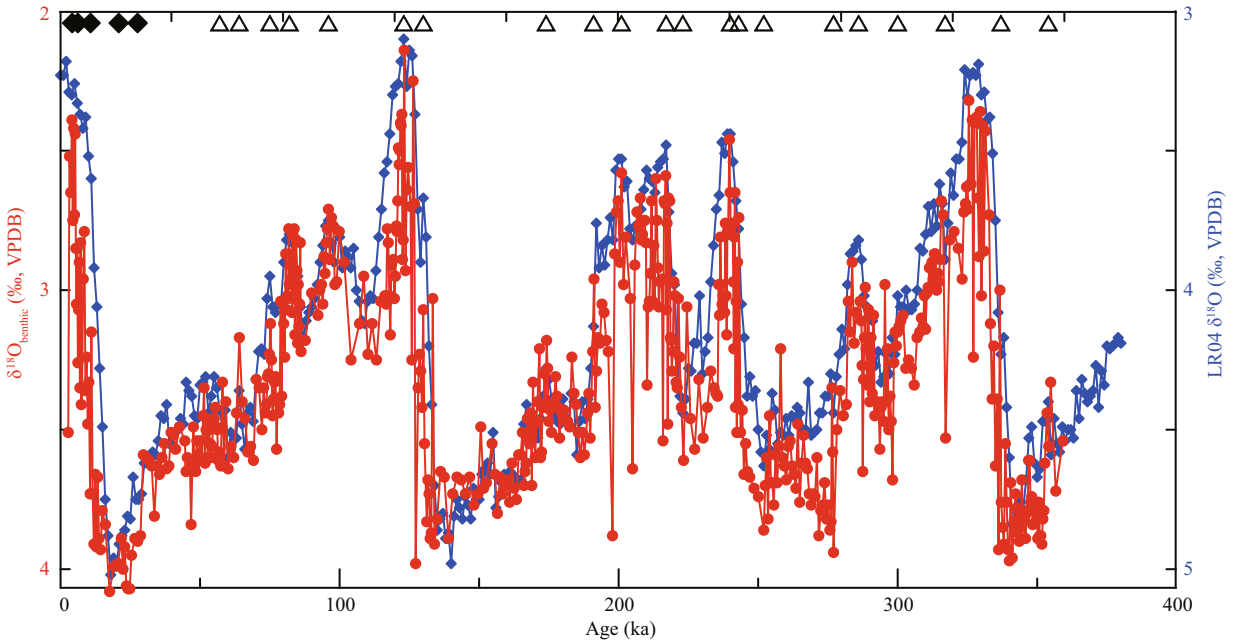

Fig.2 Age model of core KX97322-4

Benthic foraminiferal $\delta^{18}O$ record (*C. wuellerstorfi*) of core KX97322-4, compared with the benthic stack LR04 (Lisiecki and Raymo, 2005). The 5 AMS ^{14}C ages (black diamonds) and 21 benthic foraminiferal tie points (white triangles), indicated in the figure, were used in the Match 2.3.1 software (Lisiecki and Raymo, 2005).

Table 1 Radiocarbon ages used to construct the chronology of KX97322-4

Sample number	Depth (cm)	^{14}C age (yr BP)	Error (yr)	Calendar age (cal. yr BP)
973-6	5–6	4 120	±25	4 177
973-14	13–14	5 770	±25	6 203
973-27	26–27	9 820	±35	10 739
973-40	39–40	17 700	±65	20 855
973-50	49–50	23 800	±85	27 597

Mg/Ca(mmol/mol)=*B*exp[*AT*(°C)] (Lea et al., 2000), where *A* and *B* represent the sensitivity of the Mg/Ca of the shell to temperature and species differences, respectively (Anand et al., 2003). We used parameters based on the sediment trap time series to reconstruct the SST, as below:

Mg/Ca (mmol/mol)=0.34exp[0.102×SST(°C)],

[0.34(±0.08); 0.102(±0.010)] (Anand et al., 2003).

The standard error of this equation, when fitted to Pacific core-tops values, was estimated at ±1.2°C. It summarizes the results of previous research and considers other impact factors, such as different cleaning methods and differences between laboratories (Anand et al., 2003).

The oxygen isotope of calcite ($\delta^{18}O_c$) is influenced by both the ambient SST and oxygen isotopic ratio of seawater ($\delta^{18}O_{sw}$). The $\delta^{18}O_{sw}$ is controlled mainly by local hydrology and global ice volume change (Lea et al., 2002). Therefore, we can remove the influence of water temperature from $\delta^{18}O$ to obtain $\delta^{18}O_{sw}$, which mainly represents sea surface salinity (SSS) (Rosenthal et al., 2003; Stott et al., 2004). We used the empirical relationship (below) between temperature and $\delta^{18}O$ to calculate the local $\delta^{18}O_{sw}$:

$$\delta^{18}O_{sw}=(SST_{Mg/Ca}-16.5+4.8\times\delta^{18}O_{G.ruber})/4.8+0.27$$

(Bemis et al., 1998; Thunell et al., 1999).

2.4 Radiocarbon dating and age model

Accelerator mass spectrometer (AMS) ^{14}C dates were determined on samples of planktic foraminifera *Globigerinoides sacculifer* (with sac) and measured at the NOSAMS Facility, WHOI, USA. AMS ^{14}C ages were converted to calendar ages using the MARINE13 calibration curve of the CALIB 7.0.2 program (Stuiver and Reimer, 1993) with a reservoir age of 400 years (Table 1). The age model (Fig.2) was obtained by comparing the $\delta^{18}O$ curve of the benthic foraminifera *C. wuellerstorfi* with the LR04 benthic reference curve (Lisiecki and Raymo, 2005) using Match 2.3.1 software (Lisiecki and Lisiecki, 2002). This was done in combination with 19 tie points, 5 AMS ^{14}C ages, and the LAD (last appearance datum) of *G. ruber* (pink), which is dated at ~120 ka in the Indian and Pacific oceans (Thompson et al., 1979). According to the age model, the sedimentation rate varied from 0.39 to 4.95 cm/kyr, with a mean value of 1.75 cm/kyr.

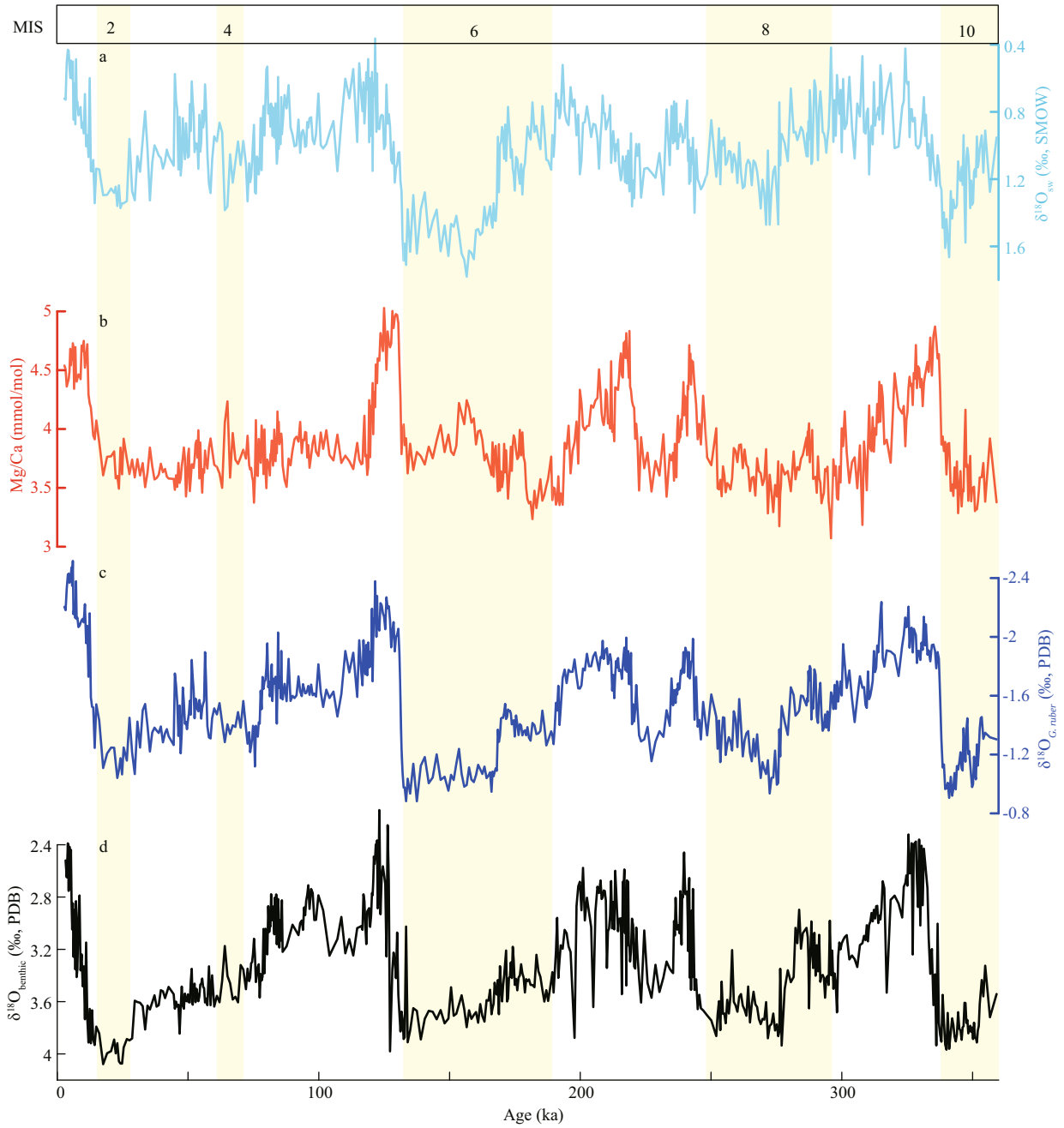

Fig.3 Variation of proxies of core KX97322-4 over the past 360kyr

a. the $\delta^{18}O_{sw}$ (‰, SMOW) record of core KX97322-4; b. the Mg/Ca (mmol/mol)-SST (°C) record of core KX97322-4; c. the $\delta^{18}O$ (‰, PDB) record of the planktic foraminifera *G. ruber*; d. the $\delta^{18}O$ (‰, PDB) record of the benthic foraminifera *C. wuellerstorfi*. Yellow vertical bars indicate glacial periods.

2.5 Periodic analysis

To extract the significant periodicities documented in the proxy records, spectral analyses were performed using the Past 3.06 software (Hammer et al., 2001) and the REDFIT procedure (Schulz and Mudelsee, 2002), which was projected to the unevenly spaced time series. In this study, window=rectangle, and oversample=10.

3 RESULT

The oxygen isotope values of the benthic foraminifera *C. wuellerstorfi* ($\delta^{18}O_{benthic}$) range between 2.14‰ and 4.08‰ for the past 360 kyr, presenting very clear glacial-interglacial cycles (Fig.2). Similarly, the $\delta^{18}O_c$ values of the planktic foraminifera *G. ruber* ($\delta^{18}O_{G.\ ruber}$) also exhibit similar glacial-interglacial cycles (Fig.3), ranging from

-2.52‰ to -0.88‰ (average: -1.57‰) during the past 360 kyr. The heaviest $\delta^{18}O$ (-0.88‰) was in MIS 6 (137.5 ka BP) and the lightest $\delta^{18}O$ (-2.52‰) was in the Holocene (5.5 ka BP). The largest amplitude occurred in MIS6/MIS5 (133.4–130.4 ka BP), when $\delta^{18}O_{G.\ ruber}$ changed from -0.88‰ to -2.05‰.

The Mg/Ca values of the planktic foraminifera *G. ruber* range between 3.07 and 5.03 mmol/mol, with a core-top value of 4.54 mmol/mol (Fig.3b). The calculated SST record indicates a core-top (average of the top five intervals) SST of 29.02±0.22°C (±0.2 SD), which is in accordance with the modern annual average SST of 29.36°C at this position (Schlitzer, 2015). As *G. ruber* generally inhabit upper-level water (depth: 0–25 m) (Sadekov et al., 2009) and because seasonal SST variation is negligible at the center of WPWP (Kawahata et al., 2002; Mohtadi et al., 2009), the calcification temperature of *G. ruber* mainly represents the annual average SST variation. Generally, SST changes demonstrate clear glacial-interglacial cycles similar to the $\delta^{18}O_c$ change during the past four terminations (Fig.3). In MIS 2 (28.64–16.05 ka BP), the lowest SST of 26.4°C appeared at 23.58 ka BP, lower than the core top SST by 2.9±0.7°C, corresponding to nearby records in the WPWP (Lea et al., 2000; de Garidel-Thoron et al., 2007; Tripati et al., 2014). Since the last termination, the minimum temperature has been 26.02°C at 75.2 ka BP and the maximum temperature has been 30.36°C at 125.0 ka BP. Within the last four terminations, SSTs have shown rapid variations, climbing from a minimum value to a maximum value over a period of only 5 000–6 000 years. However, the subsequent cooling could last for 20–40 thousand years (Fig.3b). In the last glacial period, SST fluctuated wildly within the range of approximately 26–28°C.

The calculated core-top $\delta^{18}O_{sw}$ is (0.5±0.07)‰, which is similar to the modern $\delta^{18}O_{sw}$ in the central WPWP (Schmidt et al., 1999) and mainly reflects local SSS variation (Schmidt and Spero, 2011). Over the past 360 kyr, the SSS values were high in glacial periods and low in interglacial periods, fitting well with the global mean $\delta^{18}O_{sw}$ variation (Waelbroeck et al., 2002) (Fig.3a).

4 DISCUSSION

4.1 La Niña-like state during glacial periods

Comparison of the proxies between the WPWP and EPCT (Fig.4) indicated similar $\delta^{18}O_{G.\ ruber}$ values of between -2.5‰ and 0‰ during the interglacial periods (Lea et al., 2000; Pena et al., 2008), whereas, they diverged widely in the glacial periods. The Mg/Ca-SST data show that the WPWP SST was always higher than that of the EPCT during the last 360 kyr (Figs.4, 5), although the patterns of variation in both regions were similar.

Based on the NOAA Extended Reconstructed SST of 1950–2015 (Version 4, in situ only), the annual mean zonal SST gradient (ΔSST) between the WPWP and EPCT is presently about 3.3°C (Fig.1). During all the glacial periods, the ΔSST displayed larger values than at present, which is indicative of an almost La Niña-like state (Fig.4d). During the LGM, the ΔSST was 3.8±0.5°C, suggesting an evident La Niña-like state, which is consistent with other paleotemperature and thermocline gradient reconstructions (Martínez et al., 2003; Dubois et al., 2009; Rincón-Martínez et al., 2010; Bolliet et al., 2011; Regoli et al., 2015) and simulated results (Clement et al., 1999; Hewitt et al., 2003; Kim et al., 2003). The presence of massive high-latitude ice sheets could alter the general circulation of the atmosphere and intensify the Hadley circulation (Kim and Lee, 2001a, b; Timmermann et al., 2004). However, some contradictory results have suggested that the LGM was inclined toward an El Niño-like state (Koutavas et al., 2002; Stott et al., 2002; Koutavas and Lynch-Stieglitz, 2003;Visser et al., 2003; de Garidel-Thoron et al., 2007). It should be noted that most of those studies, which were based on short time scale records, have significant biases in interpretation owing to the lack of consideration of the long-term mean state of the tropical Pacific (Rosenthal and Broccoli, 2004).

During the last 360 kyr, the zonal SSS gradient between the WPWP and EPCT was strong in MIS 2, MIS 4, and MIS 6, as shown by the variation of $\Delta\delta^{18}O_{sw}$ (0.80‰, 0.73‰, and 0.81‰, respectively). Nevertheless, the $\Delta\delta^{18}O_{sw}$ in MIS 8 was unlike the other cold periods and it showed almost an inverse pattern (Fig.5c). The differences in the $\delta^{18}O_{sw}$ values in the EPCT in MIS 8 and MIS 10 (Fig.4c) could be attributed to latitudinal differences (Koutavas and Lynch-Stieglitz, 2003). Additionally, with regard to the location of our site, El Niño events could also enhance the precipitation in these areas (Delcroix and Picaut, 1998; Stott et al., 2002; Chen et al., 2004; Schmidt and Spero, 2011). This means the results have certain ambiguity. Nevertheless, $\Delta\delta^{18}O_{sw}$ was high in the glacial periods and low in the interglacial periods and this variation has been interpreted as reflecting an increase in rainfall in the WPWP induced

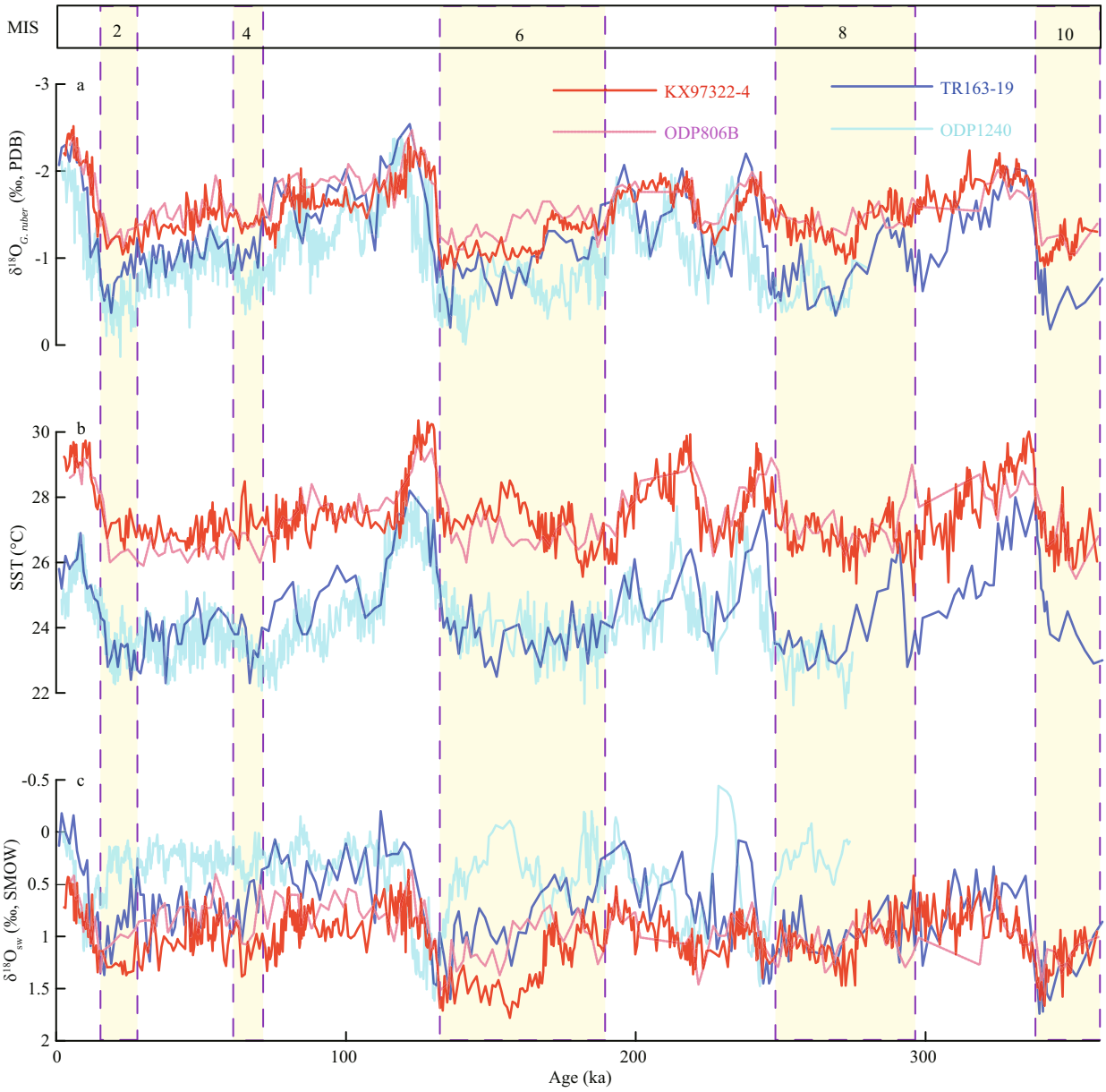

Fig.4 Comparison of the records of the WPWP and EPCT, showing $\delta^{18}O$ (‰, PDB), SST (°C), and $\delta^{18}O_{sw}$ (‰, SMOW) records from core KX97322-4 (red), ODP806B (pink), TR163-19 (blue) (Lea et al., 2000), and ODP1240 (azure) (Pena et al., 2008)

by a La Niña-like state (Lea et al., 2000). A strong zonal SST gradient contributes to the intensity of the Walker cell, strengthens the trade winds, and transports additional water vapor to the WPWP, enhancing its precipitation (Andreasen and Ravelo, 1997; Lea et al., 2000). A multiproxy assessment of the western equatorial Pacific hydrography has indicated the possibility of a slight decrease in SSS in the WPWP during glacial periods (de Garidel-Thoron et al., 2007).

Some evidence has shown that the thermocline did not deepen in the WPWP in glacial periods (Sagawa et al., 2012; Zhang et al., 2013). During glacial periods, the decrease of equatorial SST would weaken ocean stratification (Pisias and Mix, 1997; Lea et al., 2000) and shoal the thermocline (Fedorov and Philander, 2000; Beaufort et al., 2001). It has been suggested that the decreased SSS was attributed to suppressed evaporation by cold surface waters and the lack of deep atmospheric convection (Sagawa et al., 2012). Other precipitation records and models have also proposed that there was no enhanced precipitation in glacial periods (Kitoh and Murakami, 2002; Partin et al., 2007). In the WPWP, the thermal center is adjacent to the salinity front and it does not coincide with the center of precipitation (Fig.1) (Delcroix and Picaut,

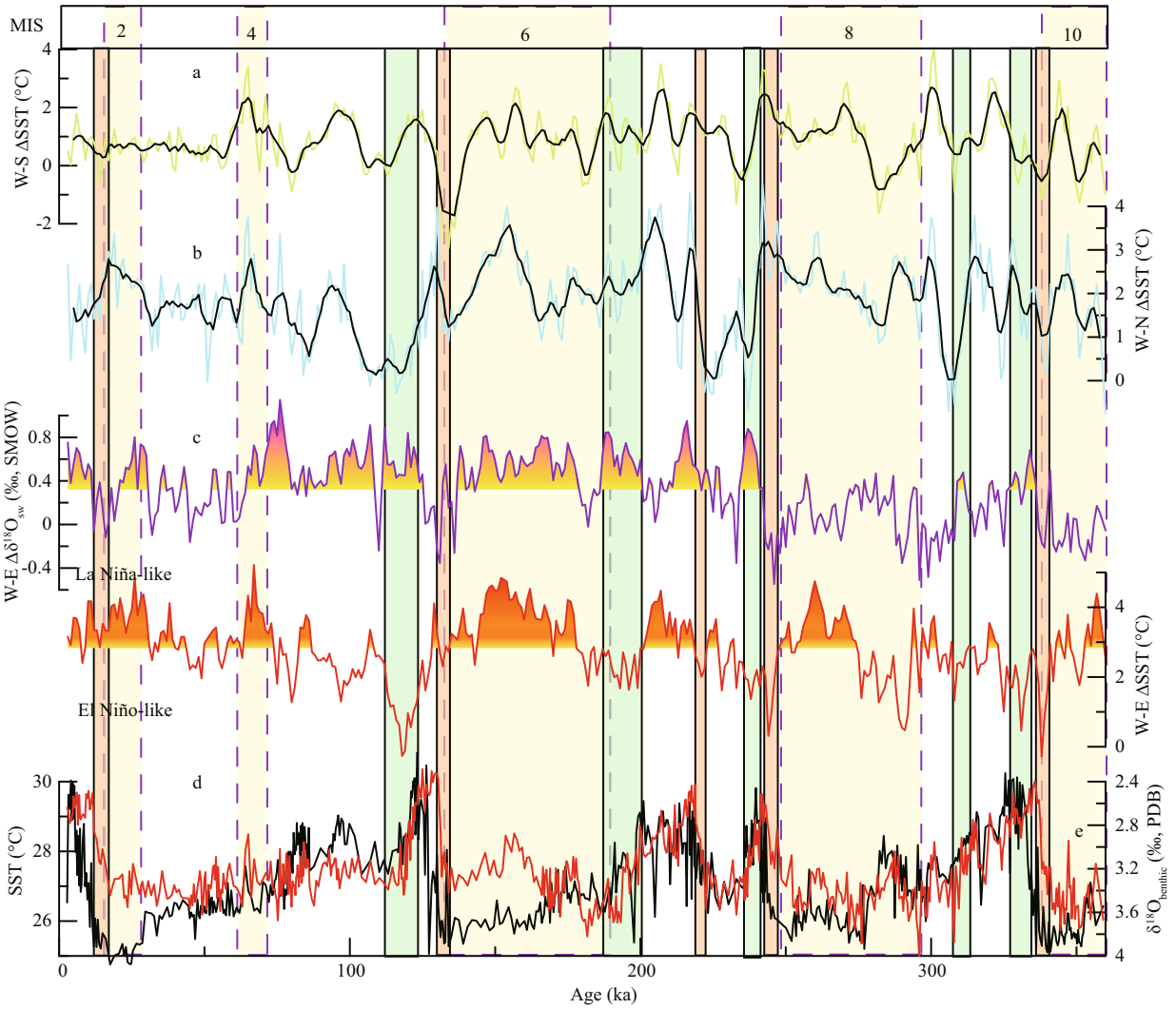

Fig.5 Differences between the records of the central WPWP and other sea areas

(a) and (b) the southern and northern edge of the WPWP, respectively, (c) and (d) the EPCT. The difference is calculated by linear interpolation with a window of 1 000 years. Yellow bars indicate glacial periods and peach and green bars indicate rapid warming and cooling periods, respectively. Shadows in (c) and (d) indicate the difference exceeds the modern mean difference. (e) the $\delta^{18}O_{benthic}$ (‰, PDB) records (black) and SST (°C) records (red) of KX97322-4.

1998; Chen et al., 2004). In glacial periods, the position and extent of the WPWP will have changed and thus, different proxies in diverse situations might record contradictory information.

4.2 Synchronic change of zonal and meridional SST gradients

The SST gradient was large between our site and the northern edge of the WPWP (Wang and Li, 2012) during the LGM and those periods when the tropical Pacific was in La Niña-like states (Fig.5b), which could mean that the extent of the WPWP was reduced and accompanied by enhanced Walker and Hadley circulations during the LGM. In contrast, the variations of the zonal SST gradient in the equatorial Pacific and the meridional SST gradient between the center and edge of the WPWP were almost identical during the last 360 kyr, consistent with a reconstruction based on a much longer time scale (Fedorov et al., 2015). Moreover, an analysis of the quantitative change in nanoplankton communities preserved in nine deep-sea cores has indicated that primary production along the equatorial Pacific was enhanced during the LGM (Beaufort et al., 2001). This could probably be attributed to enhanced upwelling in the EEP during a La Niña-like state (Beaufort et al., 2001; Sarmiento et al., 2004) and to greater input of eolian dust due to a reinforced East Asian Winter Monsoon (Zhang et al., 2007; Li et al., 2010; Zhou et al., 2011; Xiong et al., 2013, 2015). Both phenomena would provide additional nutrients to facilitate primary production.

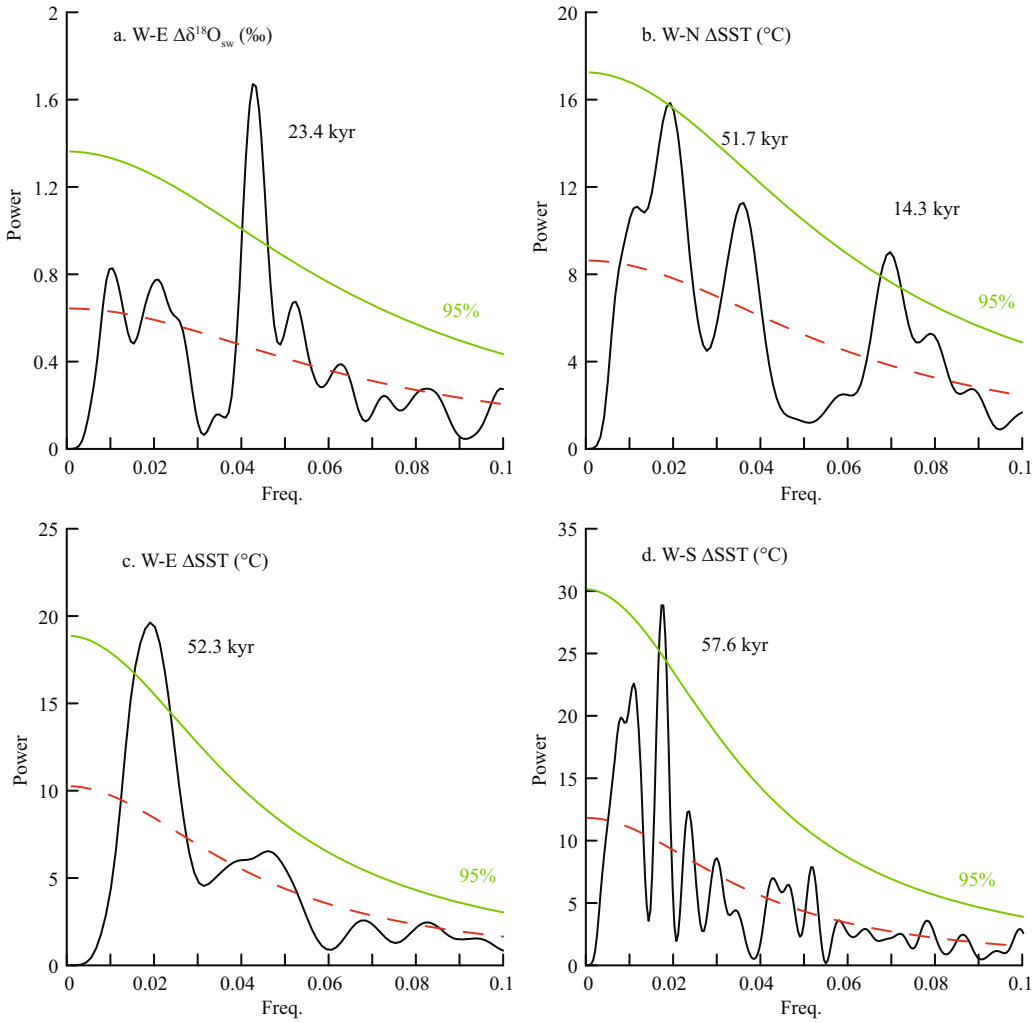

Fig.6 Spectral analysis of the proxies used in this study

Compared with our results, an Mg/Ca-SST reconstruction from the Gulf of Papua on the southern edge of the WPWP (Regoli et al., 2015), showed that ΔSST was smaller than the modern annual average ΔSST (1.98°C) (Schlitzer, 2015) or even almost zero during the LGM (Fig.5a). This could be indicative of a shift to the south of a shrinking WPWP, which might have caused an early retreat of the southern tropical glaciers (Smith et al., 2005). This phenomenon could be explained by the mechanism of a seesaw or a lead-lag between the Southern and Northern hemispheres driven by precession-antiphase-induced insolation asymmetry (Berger, 1978).

Spectral analysis of the $\delta^{18}O_{sw}$ difference between the WPWP and EPCT revealed a significant 23.4 ka cycle (Fig.6a) related to the insolation variation over the equator controlled by precession. However, the zonal SST gradient mainly has a ~52 ka cycle (Fig.6c), which has been interpreted as the heterodyne frequency of the main orbital cycles (precession and obliquity) (Clemens and Prell, 1991; Clemens et al., 1991). It means that the zonal SST gradient is not only related to variations of insolation over the equator but it is also indirectly influenced by high latitude. A ~52 ka cycle of the meridional SST gradient confirms the close relationship between the zonal and meridional SST gradient variation mentioned above, and the teleconnection between high and low latitudes (Fig.6b). Compared with the SST records of the southwest Pacific (Tachikawa et al., 2009), the SST gradient also shows a ~57 ka cycle (Fig.6d). Proxies of the Indian Ocean summer monsoon from the Arabian Sea have revealed a similar periodicity, which has been explained as the effect of large-amplitude insolation events produced by the combination of obliquity and precession (Clemens and Prell, 1991). The zonal and meridional SST gradients might have the same original driver

and they might be tied to the variation of the monsoon in low latitudes. Consequently, in glacial periods, the meridional SST gradient was strong (Fig.5b), meaning there must have been a strong Walker circulation over equator and a strong Hadley circulation in the western Pacific. Furthermore, the East Asian Winter Monsoon would have been dominant and the La Niña-like state in the tropic would have been sustained, maintaining the ice age.

4.3 El Niño-like state during rapidly changing periods

Previous research has discussed super-ENSO events in interglacial periods (Beaufort et al., 2001; Rincón-Martínez et al., 2010; Zhang et al., 2015). Nevertheless, interglacial periods defined by marine isotopes are not consistent with SST variations in the tropical Pacific (Fig.4), i.e., tropical SSTs during such periods are not as stable as in glacial periods. The real warm time in an interglacial period generally persists for 10–30 kyr, and it is always combined with a subsequent cooling process that involves a sequence of global fluctuations. Accordingly, an interglacial period should not be regarded as a single entity, as discussed in previous studies.

The comparison of the proxies of the WPWP and EPCT revealed an interesting point in the rapidly cooling stages of the interglacial periods (i.e., 112–124, 187–200, 235–240, and 328–334 ka) (Fig.5). The zonal SST gradients assumed El Niño-like states, zonal $\delta^{18}O_c$ gradients, relatively small meridional SST gradients, and relatively large zonal $\delta^{18}O_{sw}$ gradients. This indicated that the Walker and Hadley circulations were weakened and that the SSS difference increased because of reduced precipitation in the WPWP. This phenomenon can also be seen in the terminations, when the SST was rising quickly, mean zonal SST and $\delta^{18}O_{sw}$ gradients were relatively weak, and meridional SST gradients were increasing gradually from relatively low values (Fig.5). The contrast between the SST of the equatorial Indian Ocean and EEP also showed an extremely low value in the terminations (Saraswat et al., 2007). This was probably because there was more water vapor and energy transported to the extratropical regions, which enhanced the local SSS of the WPWP (Kukla et al., 2002). In the terminations, the carbon isotope minimum events in the WPWP also recorded enhanced upwelling (Qiu et al., 2014b), which has been taken as indicative of a shoaling thermocline (Pena et al., 2008). It could also be taken to indicate El Niño-like conditions, while the strength of the last four El Niño-like episodes in the four terminations was decreasing.

These episodes of rapid change are contrary to the LGM when the SST in the WPWP remained relatively stable. During episodes of rapid change, the amplitude of the SST variation in the EPCT was larger than in the WPWP. The weakened zonal SST gradients might have arisen because of a smaller and less intense WPWP and/or greater SST change in the equatorial and coastal upwelling zones of the EPCT (Rodbell et al., 1999). Modern simulation studies suggest that rapid global warming would generate more or even double the number of El Niño events (Cai et al., 2014) caused by the situation where surface warming of the EPCT is faster than in the surrounding sea areas and the WPWP (Knutson and Manabe, 1995; Tett, 1995; Sun, 2003). This sensibility would make EPCT warming lead the WPWP during deglaciation. The simulations also indicate that the ITCZ would move to the rapidly warming eastern equator and promote frequent atmospheric convection (Lengaigne and Vecchi, 2010; Xie et al., 2010; Tokinaga et al., 2012). Modern observations have proposed that El Niño could be the primary mechanism via which the tropical Pacific transports heat poleward (Sun, 2003). Thus, it is beneficial for the melting of glaciers in the mid- and high latitudes (Cane, 1998; Clement et al., 1999).

Summer insolation in the tropics during deglaciation was evidently intensified and it promoted rapid warming in equatorial regions, especially in the EPCT. This compensation to the weakened zonal SST gradient could mean an El Niño-like state existed in the tropical Pacific during periods of SST warming, promoting global warming. The El Niño-like state in rapidly cooling stages of interglacial periods could have arisen from the lag of cooling in the EPCT compared with the WPWP. We hypothesize an inter-restricted relationship between the WPWP and EPCT that controls the nature of the variation of SST. When insolation strengthens over equatorial regions, WPWP expansion accelerates the warming of the EPCT, although the EPCT simultaneously constrains the WPWP warming. As insolation weakens, EPCT cooling is restrained by the influence of the WPWP through an equatorial undercurrent, while WPWP cooling is promoted by the influence of surface cold waters from the EPCT. This mechanism within the tropical Pacific could influence global variations during times of rapid change.

5 CONCLUSION

The $\delta^{18}O$ and Mg/Ca analyses of foraminiferal calcite in core KX97322-4 reflect the variations of SST and SSS in the WPWP during the last 360 kyr. Comparison between our data and other records from the Pacific showed that during the LGM and other glacial periods, when the SST was relatively stable, the tropical Pacific experienced a La Niña-like state and that the Walker and Hadley circulations were enhanced. In rapidly changing periods, whether cooling stages in interglacial periods or warming stages in deglaciations, the El Niño-like condition would appear in the tropical Pacific. In consequence of the sensitivity of the EPCT and the inertia of the WPWP, we hypothesize an inter-restricted relationship between the WPWP and EPCT that controls the variation of SST. By spectral analysis of the proxies, we established a close relationship between the zonal and meridional SST gradient variations. The tropical Pacific plays a vital role in global climate change and further research of this area is required.

6 ACKNOWLEDGEMENT

The authors are grateful to the editor and the anonymous reviewers for their valuable advice.

References

An Z S. 2000. The history and variability of the East Asian paleomonsoon climate. *Quaternary Science Reviews*, **19**(1-5): 171-187.

Anand P, Elderfield H, Conte M H. 2003. Calibration of Mg/Ca thermometry in planktonic foraminifera from a sediment trap time series. *Paleoceanography*, **18**(2): 1 050.

Andreasen D J, Ravelo A C. 1997. Tropical Pacific ocean thermocline depth reconstructions for the last glacial maximum. *Paleoceanography*, **12**(3): 395-413.

Barker S, Greaves M, Elderfield H. 2003. A study of cleaning procedures used for foraminiferal Mg/Ca paleothermometry. *Geochemistry*, *Geophysics*, *Geosystems*, **4**(9): 8 407.

Beaufort L, de Garidel-Thoron T, Mix A C, Pisias N G. 2001. ENSO-like forcing on oceanic primary production during the Late Pleistocene. *Science*, **293**(5539): 2 440-2 444.

Bemis B E, Spero H J, Bijma J, Lea D W. 1998. Reevaluation of the oxygen isotopic composition of planktonic foraminifera: experimental results and revised paleotemperature equations. *Paleoceanography*, **13**(2): 150-160.

Berger A. 1978. Long-term variations of caloric insolation resulting from the earth's orbital elements. *Quaternary Research*, **9**(2): 139-167.

Bolliet T, Holbourn A, Kuhnt W, Laj C, Kissel C, Beaufort L, Kienast M, Andersen N, Garbe-Schönberg D. 2011. Mindanao Dome variability over the last 160 kyr: episodic glacial cooling of the West Pacific Warm Pool. *Paleoceanography*, **26**(1): PA1208.

Cai W, Borlace S, Lengaigne M, van Rensch P, Collins M, Vecchi G, Timmermann A, Santoso A, McPhaden M J, Wu L X, England M H, Wang G J, Guilyardi E, Jin F F. 2014. Increasing frequency of extreme El Niño events due to greenhouse warming. *Nature Climate Change*, **4**(2): 111-116.

Cane M A. 1998. Climate change: a role for the tropical Pacific. *Science*, **282**(5386): 59-61.

Carré M, Sachs J P, Purca S, Schauer A J, Braconnot P, Falcón R A, Julien M, Lavallée D. 2014. Holocene history of ENSO variance and asymmetry in the eastern tropical Pacific. *Science*, **345**(6200): 1 045-1 048.

Chen G, Fang C Y, Zhang C Y, Chen Y. 2004. Observing the coupling effect between warm pool and "rain pool" in the Pacific Ocean. *Remote Sensing of Environment*, **91**(2): 153-159.

Clemens S C, Prell W L. 1991. Late Quaternary forcing of Indian Ocean summer-monsoon winds: a comparison of Fourier model and general circulation model results. *Journal of Geophysical Research*: *Atmospheres*, **96**(D12): 22 683-22 700.

Clemens S, Prell W, Murray D, Shimmield G, Weedon G. 1991. Forcing mechanisms of the Indian Ocean monsoon. *Nature*, **353**(6346): 720-725.

Clement A C, Seager R, Cane M A. 1999. Orbital controls on the El Niño/southern oscillation and the tropical climate. *Paleoceanography*, **14**(4): 441-456.

Cobb K M, Westphal N, Sayani H R, Watson J T, Di Lorenzo E, Cheng H, Edwards R L, Charles C D. 2013. Highly variable El Niño-southern oscillation throughout the holocene. *Science*, **339**(6115): 67-70.

Cronin M F, McPhaden M J. 1997. The upper ocean heat balance in the western equatorial Pacific warm pool during September-December 1992. *Journal of Geophysical Research*: *Oceans*, **102**(C4): 8 533-8 553.

Crowley T J. 2000. CLIMAP SSTs re-revisited. *Climate Dynamics*, **16**(4): 241-255.

de Garidel-Thoron T, Rosenthal Y, Beaufort L, Bard E, Sonzogni C, Mix A C. 2007. A multiproxy assessment of the western equatorial Pacific hydrography during the last 30 kyr. *Paleoceanography*, **22**(3): PA3204.

Delcroix T, Picaut J. 1998. Zonal displacement of the western equatorial Pacific "fresh pool". *Journal of Geophysical Research*: *Oceans*, **103**(C1): 1 087-1 098.

Dubois N, Kienast M, Normandeau C, Herbert T D. 2009. Eastern equatorial Pacific cold tongue during the Last Glacial Maximum as seen from alkenone paleothermometry. *Paleoceanography*, **24**(4): PA4207.

Fedorov A V, Burls N J, Lawrence K T, Peterson L C. 2015. Tightly linked zonal and meridional sea surface temperature gradients over the past five million years. *Nature Geoscience*, **8**(12): 975-980.

Fedorov A V, Philander S G. 2000. Is El Niño changing. *Science*, **288**(5473): 1 997-2 002.

Ford H L, Ravelo A C, Polissar P J. 2015. Reduced El Niño-southern oscillation during the last glacial maximum. *Science*, **347**(6219): 255-258.

Hammer Ø, Harper D A T, Ryan P D. 2001. PAST: palaeontological statistics software package for education and data analysis. *Palaeontologia Electronica*, **4**(1): 1-9.

Hewitt C, Stouffer R, Broccoli A, Mitchell J, Valdes P J. 2003. The effect of ocean dynamics in a coupled GCM simulation of the Last Glacial Maximum. *Climate Dynamics*, **20**(2-3): 203-218.

Jin F F. 1996. Tropical ocean-atmosphere interaction, the Pacific cold tongue, and the El Niño-southern oscillation. *Science*, **274**(5284): 76-78.

Kawahata H, Nishimura A, Gagan M K. 2002. Seasonal change in foraminiferal production in the western equatorial Pacific warm pool: evidence from sediment trap experiments. *Deep Sea Research Part II*: *Topical Studies in Oceanography*, **49**(13-14): 2 783-2 800.

Kim H K, Lee S. 2001a. Hadley Cell Dynamics in a primitive equation model. Part I: axisymmetric flow. *Journal of the Atmospheric Sciences*, **58**(19): 2 845-2 858.

Kim H K, Lee S. 2001b. Hadley cell dynamics in a primitive equation model. Part II: nonaxisymmetric flow. *Journal of the Atmospheric Sciences*, **58**(19): 2 859-2 871.

Kim S J, Flato G M, Boer G J. 2003. A coupled climate model simulation of the Last Glacial Maximum, Part 2: approach to equilibrium. *Climate Dynamics*, **20**(6): 635-661.

Kitoh A, Murakami S. 2002. Tropical Pacific climate at the mid-Holocene and the Last Glacial Maximum simulated by a coupled ocean-atmosphere general circulation model. *Paleoceanography*, **17**(3): 19-1-19-13.

Knutson T R, Manabe S. 1995. Time-mean response over the tropical Pacific to increased CO_2 in a coupled ocean-atmosphere model. *Journal of Climate*, **8**(9): 2 181-2 199.

Koutavas A, Lynch-Stieglitz J, Marchitto Jr T M, Sachs J P. 2002. El Niño-like pattern in ice age tropical Pacific sea surface temperature. *Science*, **297**(5579): 226-230.

Koutavas A, Lynch-Stieglitz J. 2003. Glacial-interglacial dynamics of the eastern equatorial Pacific cold tongue-Intertropical Convergence Zone system reconstructed from oxygen isotope records. *Paleoceanography*, **18**(4): 1089.

Kukla G J, Clement A C, Cane M A, Gavin J E, Zebiak S E. 2002. Last interglacial and early glacial ENSO. *Quaternary Research*, **58**(1): 27-31.

Lea D W, Martin P A, Pak D K, Spero H J. 2002. Reconstructing a 350 ky history of sea level using planktonic Mg/Ca and oxygen isotope records from a Cocos Ridge core. *Quaternary Science Reviews*, **21**(1-3): 283-293.

Lea D W, Pak D K, Spero H J. 2000. Climate impact of late quaternary equatorial Pacific sea surface temperature variations. *Science*, **289**(5485): 1 719-1 724.

Leduc G, Vidal L, Tachikawa K, Bard E. 2009. ITCZ rather than ENSO signature for abrupt climate changes across the tropical Pacific. *Quaternary Research*, **72**(1): 123-131.

Lengaigne M, Vecchi G. 2010. Contrasting the termination of moderate and extreme El Niño events in coupled general circulation models. *Climate Dynamics*, **35**(2-3): 299-313.

Li C Y, Mu M Q, Zhou G Q. 1999. The variation of warm pool in the equatorial western pacific and its impacts on climate. *Advances in Atmospheric Sciences*, **16**(3): 378-394.

Li T G, Zhao J T, Sun R T, Chang F M, Sun H J. 2010. The variation of upper ocean structure and paleoproductivity in the Kuroshio source region during the last 200 kyr. *Marine Micropaleontology*, **75**(1-4): 50-61.

Lisiecki L E, Lisiecki P A. 2002. Application of dynamic programming to the correlation of paleoclimate records. *Paleoceanography*, **17**(4): 1-1-1-12.

Lisiecki L E, Raymo M E. 2005. A Pliocene-Pleistocene stack of 57 globally distributed benthic $\delta^{18}O$ records. *Paleoceanography*, **20**(1): PA1003.

MARGO Project Members. 2009. Constraints on the magnitude and patterns of ocean cooling at the Last Glacial Maximum. *Nature Geoscience*, **2**(2): 127-132.

Martínez I, Keigwin L, Barrows T T, Yokoyama Y, Southon J. 2003. La Niña-like conditions in the eastern equatorial Pacific and a stronger Choco jet in the northern Andes during the last glaciation. *Paleoceanography*, **18**(2): 1 033.

Mathien-Blard E, Bassinot F. 2009. Salinity bias on the foraminifera Mg/Ca thermometry: correction procedure and implications for past ocean hydrographic reconstructions. *Geochemistry*, *Geophysics*, *Geosystems*, **10**(12): Q12011.

Mohtadi M, Steinke S, Groeneveld J, Fink H G, Rixen T, Hebbeln D, Donner B, Herunadi B. 2009. Low-latitude control on seasonal and interannual changes in planktonic foraminiferal flux and shell geochemistry off south Java: a sediment trap study. *Paleoceanography*, **24**(1): PA1201.

Oppo D W, Schmidt G A, LeGrande A N. 2007. Seawater isotope constraints on tropical hydrology during the Holocene. *Geophysical Research Letters*, **34**(13): L13701.

Palmer T N, Mansfield D A. 1984. Response of two atmospheric general circulation models to sea-surface temperature anomalies in the tropical East and West Pacific. *Nature*, **310**(5977): 483-485.

Partin J W, Cobb K M, Adkins J F, Clark B, Fernandez D P. 2007. Millennial-scale trends in west Pacific warm pool hydrology since the Last Glacial Maximum. *Nature*, **449**(7161): 452-455.

Pena L D, Cacho I, Ferretti P, Hall M A. 2008. El Niño-Southern Oscillation-like variability during glacial terminations and interlatitudinal teleconnections. *Paleoceanography*, **23**(3): PA3101.

Pisias N G, Mix A C. 1997. Spatial and temporal oceanographic variability of the eastern equatorial Pacific during the Late Pleistocene: evidence from radiolaria microfossils. *Paleoceanography*, **12**(3): 381-393.

Qiu X H, Li T G, Chang F M, Nan Q Y, Xiong Z F, Sun H J. 2014a. Sea surface temperature and salinity reconstruction

based on stable isotopes and Mg/Ca of planktonic foraminifera in the western Pacific Warm Pool during the last 155 ka. *Chinese Journal of Oceanology and Limnology*, **32**(1): 187-200.

Qiu X H, Li T G, Nan Q Y, Gong H M. 2014b. Carbon isotope minimum events in the northern margin of western Pacific Warm Pool since during the past 150 ka. *Marine Sciences*, **38**(11): 116-121. (in Chinese with English abstract)

Ravelo A C, Fairbanks R G, Philander S G H. 1990. Reconstructing tropical atlantic hydrography using planktontic foraminifera and an ocean model. *Paleoceanography*, **5**(3): 409-431.

Regoli F, de Garidel-Thoron T, Tachikawa K, Jian Z M, Ye L M, Droxler A W, Lenoir G, Crucifix M, Barbarin N, Beaufort L. 2015. Progressive shoaling of the equatorial Pacific thermocline over the last eight glacial periods. *Paleoceanography*, **30**(5): 439-455.

Rincón-Martínez D, Lamy F, Contreras S, Leduc G, Bard E, Saukel C, Blanz T, Mackensen A, Tiedemann R. 2010. More humid interglacials in Ecuador during the past 500 kyr linked to latitudinal shifts of the equatorial front and the Intertropical Convergence Zone in the eastern tropical Pacific. *Paleoceanography*, **25**(2): PA2210.

Rodbell D T, Seltzer G O, Anderson D M, Abbott M B, Enfield D B, Newman J H. 1999. An ~15,000-year record of El Niño-driven alluviation in southwestern ecuador. *Science*, **283**(5401): 516-520.

Rosenthal Y, Broccoli A J. 2004. In search of paleo-ENSO. *Science*, **304**(5668): 219-221.

Rosenthal Y, Oppo D W, Linsley B K. 2003. The amplitude and phasing of climate change during the last deglaciation in the Sulu Sea, western equatorial Pacific. *Geophysical Research Letters*, **30**(8): 1428.

Sadekov A Y, Eggins S M, Klinkhammer G P, Rosenthal Y. 2010. Effects of seafloor and laboratory dissolution on the Mg/Ca composition of *Globigerinoides sacculifer* and *Orbulina universa* tests-A laser ablation ICPMS microanalysis perspective. *Earth and Planetary Science Letters*, **292**(3-4): 312-324.

Sadekov A, Eggins S M, De Deckker P, Ninnemann U, Kuhnt W, Bassinot F. 2009. Surface and subsurface seawater temperature reconstruction using Mg/Ca microanalysis of planktonic foraminifera *Globigerinoides ruber*, *Globigerinoides sacculifer*, and *Pulleniatina obliquiloculata*. *Paleoceanography*, **24**(3): PA3201.

Sagawa T, Yokoyama Y, Ikehara M, Kuwae M. 2012. Shoaling of the western equatorial Pacific thermocline during the last glacial maximum inferred from multispecies temperature reconstruction of planktonic foraminifera. *Palaeogeography*, *Palaeoclimatology*, *Palaeoecology*, **346-347**: 120-129.

Saraswat R, Nigam R, Weldeab S, Mackensen A. 2007. The tropical warm pool in the Indian Ocean and its influence on ENSO over the past 137,000 yrs BP. *Current Science*, **92**(8): 1 153-1 156.

Sarmiento J L, Gruber N, Brzezinski M A, Dunne J P. 2004. High-latitude controls of thermocline nutrients and low latitude biological productivity. *Nature*, **427**(6969): 56-60.

Schlitzer R. 2015. Ocean data view 4. http://odv.awi.de.

Schmidt G A, Bigg G R, Rohling E J. 1999. Global seawater oxygen-18 database-v1.21. p.645-654.

Schmidt M W, Spero H J. 2011. Meridional shifts in the marine ITCZ and the tropical hydrologic cycle over the last three glacial cycles. *Paleoceanography*, **26**(1): PA1206.

Schulz M, Mudelsee M. 2002. REDFIT: estimating red-noise spectra directly from unevenly spaced paleoclimatic time series. *Computers & Geosciences*, **28**(3): 421-426.

Smith J A, Seltzer G O, Farber D L, Rodbell D T, Finkel R C. 2005. Early local last glacial maximum in the tropical andes. *Science*, **308**(5722): 678-681.

Stott L, Cannariato K, Thunell R, Haug G H, Koutavas A, Lund S. 2004. Decline of surface temperature and salinity in the western tropical Pacific Ocean in the Holocene epoch. *Nature*, **431**(7004): 56-59.

Stott L, Poulsen C, Lund S, Thunell R. 2002. Super ENSO and global climate oscillations at millennial time scales. *Science*, **297**(5579): 222-226.

Stuiver M, Reimer P J. 1993. Extended ^{14}C data base and revised CALIB 3.0 ^{14}C age calibration program. *Radiocarbon*, **35**(1): 215-230.

Sun D Z. 2003. A possible effect of an increase in the warm-pool SST on the magnitude of El Niño warming. *Journal of Climate*, **16**(2): 185-205.

Tachikawa K, Vidal L, Sonzogni C, Bard E. 2009. Glacial/interglacial sea surface temperature changes in the Southwest Pacific ocean over the past 360 ka. *Quaternary Science Reviews*, **28**(13-14): 1 160-1 170.

Tett S. 1995. Simulation of El Niño-southern oscillation-like variability in a global AOGCM and its Response to CO_2 Increase. *Journal of Climate*, **8**(6): 1 473-1 502.

Thompson P R, Bé A W H, Duplessy J C, Shackleton N J. 1979. Disappearance of pink-pigmented *Globigerinoides ruber* at 120, 000 yr BP in the Indian and Pacific Oceans. *Nature*, **280**(5723): 554-558.

Thunell R, Tappa E, Pride C, Kincaid E. 1999. Sea-surface temperature anomalies associated with the 1997-1998 El Niño recorded in the oxygen isotope composition of planktonic foraminifera. *Geology*, **27**(9): 843-846.

Timmermann A, Justino F, Jin F F, Krebs U, Goosse H. 2004. Surface temperature control in the North and tropical Pacific during the last glacial maximum. *Climate Dynamics*, **23**(3-4): 353-370.

Tokinaga H, Xie S P, Deser C, Kosaka Y, Okumura Y M. 2012. Slowdown of the Walker circulation driven by tropical Indo-Pacific warming. *Nature*, **491**(7424): 439-443.

Tripati A K, Sahany S, Pittman D, Eagle R A, Neelin J D, Mitchell J L, Beaufort L. 2014. Modern and glacial tropical snowlines controlled by sea surface temperature and atmospheric mixing. *Nature Geoscience*, **7**(3): 205-209.

Visser K, Thunell R, Stott L. 2003. Magnitude and timing of temperature change in the Indo-Pacific warm pool during deglaciation. *Nature*, **421**(6919): 152-155.

Waelbroeck C, Labeyrie L, Michel E, Duplessy J C, McManus J F, Lambeck K, Balbon E, Labracherie M. 2002. Sea-level and deep water temperature changes derived from benthic foraminifera isotopic records. *Quaternary Science Reviews*, **21**(1-3): 295-305.

Wang X Y, Li B H. 2012. Sea surface temperature evolution in the western South China Sea since MIS 12 as evidenced by planktonic foraminiferal assemblages and *Globigerinoides ruber* Mg/Ca ratio. *Sicence China Earth Sciences*, **55**(11): 1 827-1 836.

Wu G P, Berger W H. 1991. Pleistocene $\delta^{18}O$ records from Ontong-Java Plateau: effects of winnowing and dissolution. *Marine Geology*, **96**(3-4): 193-209.

Xie S P, Deser C, Vecchi G A, Ma J, Teng H Y, Wittenberg A T. 2010. Global warming pattern formation: sea surface temperature and rainfall. *Journal of Climate*, **23**(4): 966-986.

Xiong Z F, Li T G, Algeo T, Doering K, Frank M, Brzezinski M A, Chang F M, Opfergelt S, Crosta X, Jiang F Q, Wan S M, Zhai B. 2015. The silicon isotope composition of *Ethmodiscus rex* laminated diatom mats from the tropical West Pacific: implications for silicate cycling during the Last Glacial Maximum. *Paleoceanography*, **30**(7): 803-823.

Xiong Z F, Li T G, Crosta X, Algeo T, Chang F M, Zhai B. 2013. Potential role of giant marine diatoms in sequestration of atmospheric CO_2 during the Last Glacial Maximum: $\delta^{13}C$ evidence from laminated *Ethmodiscus rex* mats in tropical West Pacific. *Global and Planetary Change*, **108**: 1-14.

Yan X H, Ho C R, Zheng Q N, Klemas V. 1992. Temperature and size variabilities of the western Pacific warm pool. *Science*, **258**(5088): 1 643-1 645.

Zhang J Y, Wang P X, Li Q Y, Cheng X R, Jin H Y, Zhang S Y. 2007. Western equatorial Pacific productivity and carbonate dissolution over the last 550 kyr: foraminiferal and nannofossil evidence from ODP Hole 807A. *Marine Micropaleontology*, **64**(3-4): 121-140.

Zhang S, Li T G, Chang F M, Yu Z F, Wang H X. 2015. The relationship between the Tropical Pacific precipitation and the ITCZ variation since MIS 6. *Quaternary Sciences*, **35**(2): 390-400. (in Chinese with English abstract)

Zhang S, Li T G, Chang F M, Wang H X, Xiong Z F, Yu Z F. 2013. The evolution of upper water in the center of west Pacific warm pool during the last 360kyr. *Marine Geology & Quaternary Geology*, **33**(2): 87-96. (in Chinese with English abstract)

Zhou C, Jin H Y, Jian Z M. 2011. Variations of the late quaternary paleo-productivity in the western equatorial Pacific: evidences from the elemental ratios. *Quaternary Sciences*, **31**(2): 276-283. (in Chinese with English abstract)